Journal of Materials Science: Materials in Electronics (2018) 29:9045–9051
https://doi.org/10.1007/s10854-018-8930-6

Preparation and luminescence properties of $Y_{3-y}Al_{5-x}Ga_xO_{12}:Ce^{3+}_y$ phosphors

Lipeng Jiang[1] · Xiyan Zhang[1] · Shiqi Zhu[1] · He Tang[1] · Qingxi Li[1] · Wenmin Zhang[1] · Xiaoyun Mi[1] · Liping Lu[1] · Hongwei Liu[1] · Xiuling Liu[1]

Received: 18 December 2017 / Accepted: 14 March 2018 / Published online: 17 March 2018

Abstract
$Y_{3-y}Al_{5-x}Ga_xO_{12}:Ce^{3+}_y$ phosphors were prepared by high temperature solid state reaction method. The crystal structures, the influence of Ga^{3+} concentration on the photoluminescence (PL), cathodoluminescence, thermal stability and morphology of the phosphors were studied in detail. The results indicated that diffraction angle of the samples decreased gradually with the increase of Ga^{3+} ions content in XRD pattern. The emission peak of the spectra show a progressive blue-shift, the intensity increased first and then decreased and the optimal Ga^{3+} concentration in $Y_{2.94}Al_{5-x}Ga_xO_{12}:Ce^{3+}_{0.06}$ phosphors is x = 0.75. The critical concentration of Ce^{3+} in YAGG:Ce^{3+} phosphors is affected with the ratio of Ga^{3+} to Al^{3+} and the $Y_{2.9}Al_{4.25}Ga_{0.75}O_{12}:Ce^{3+}_{0.1}$ phosphor showed the best performance on PL. However, the optimum concentration of $Y_{3-y}Al_{5-x}Ga_xO_{12}:Ce^{3+}_y$ phosphors is x = 1.5 and y = 0.04 when they were excited by cathode ray.

1 Introduction

Yttrium aluminum garnet (YAG) phosphors are an important class of materials for luminescence [1–3]. YAG crystal belongs to cubic crystal system with *Ia3d* (230) space group, the lattice parameters are a = b = c = 12.008 Å, α = β = γ = 90°, Z = 8. It possesses excellent chemical, physical and thermal stability, and is an excellent matrix for inorganic phosphor materials for lighting [4–6]. Rare-earth-doped phosphors have been used widely in field emission displays and white light-emitting diodes because of advantages such as excellent luminescent characteristics, good stability and high luminescence efficiency [7, 8].

In recent years, Ga^{3+}-substituted YAG:Ce^{3+} phosphors have attracted much attention due to their high light yield compared with YAG:Ce^{3+} phosphors [9]. However, there is rare research on the occupancy sites of Ga^{3+} and Al^{3+} in garnet structure and their effects on optical properties in large Ga^{3+} concentration range. The main reason is that it is difficulty for Ga^{3+} to occupy tetrahedral site when three or more Al^{3+} were displaced, which leads to the appearance of impurities [10]. Meanwhile, as we know, there is no research on the comparison between cathodoluminescence and photoluminescence (PL) on YAGG:Ce^{3+} phosphors.

In this paper, a series of $Y_{3-y}Al_{5-x}Ga_xO_{12}:Ce^{3+}_y$ phosphors were successfully synthesized by high temperature solid state reaction method. We solve the problem that the YAGG garnet phase is difficult to form when the amount of Ga^{3+} content is large and the optimal concentration of Ga^{3+} and Ce^{3+} in PL and cathodoluminescence was discussed in detail. What's more, the effects of Ga^{3+} concentration on the thermal quenching, fluorescence lifetime and morphology properties were discussed.

2 Experimental

Y_2O_3 (99.99%), CeO_2 (99.99%), Al_2O_3 (99.99%), Ga_2O_3 (99.99%) were used as starting materials, which were precisely weighed according to the formula $Y_{3-y}Al_{5-x}Ga_xO_{12}:Ce^{3+}_y$ with stoichiometric ratio. The appropriate amount of AlF_3 was additionally added as a fluxing agent. The raw powders were mixed, grained thoroughly and then sintered at 1500 °C for 4 h in reduction atmosphere.

Phases identification was performed by X-ray powder diffraction on a Rigaku D/max-II B diffractometer, operating at 40 kV and 20 mA, using Cu Kα radiation, (λ = 1.54056 Å). PL spectra were measured on a Hitachi F-7000 luminescence

✉ Xiyan Zhang
xiyzhang@126.com

[1] School of Material Science and Engineering, Changchun University of Science and Technology, Changchun 130022, China

spectrophotometer equipped with a 150 W xenon lamp as the excitation. The temperature-dependence PL spectra were collected on a QE Pro high performance spectrometer equipped with a heating stage (THMS600, Linkam Scientific Instruments Ltd, UK), with a xenon lamp as the excitation source. The morphology was observed by scanning electron microscopy (SEM, JSM-6701F, JEOL, Japan). Cathodoluminescence (PL) spectra were measured on a OpticZenith Elec-ray system, operating at 6 kV. The luminescence decay curves were measured using a Lecroy Wave Runner 6100 digital oscilloscope (1 GHz) with a tunable laser (pulse width = 4 ns; gate = 50 ns) as the excitation (Continuum Sunlite OPO).

3 Results and discussion

Figure 1 shows XRD patterns of the $Y_{2.94}Al_{5-x}Ga_xO_{12}:Ce^{3+}_{0.06}$ (x = 0, 0.25, 0.5, 0.75, 1, 1.5, 2, 3, 3.5, 4, 4.5, 5) phosphors, the PDF#33-0040 corresponding to the standard card of YAG ($Y_3Al_5O_{12}$) and the PDF#43-0512 is the standard card of YGG ($Y_3Ga_5O_{12}$). The results indicate that the yttrium aluminium garnet phases were successfully obtained under the conditions of different Ga^{3+} doping concentration. From the figure, we can find that the diffraction angle decreased gradually with the increase of Ga^{3+} ions content. Which can be explained by the Bragg equation $2d\sin\theta = \lambda$, the interplanar spacing d value becomes larger with the lattice expansion when Al^{3+} ions were replaced by Ga^{3+} ions (the lattice parameters of YAG are a = b = c = 12.008 Å, α = β = γ = 90°, Z = 8, and the lattice parameters of YGG are a = b = c = 12.27 Å, α = β = γ = 90°, Z = 8), the diffraction angle will decrease because of the ionic radius of Ga^{3+} is more than that of Al^{3+}, exhibits a slight shift toward to lower 2θ angles. When Al^{3+} ions were completely replaced by Ga^{3+} ions, the sample becomes YGG. Besides, the diffraction intensity of (211), (321), (521), (532) crystal plane decreased gradually and the diffraction intensity of (400), (422), (642) increased simultaneously.

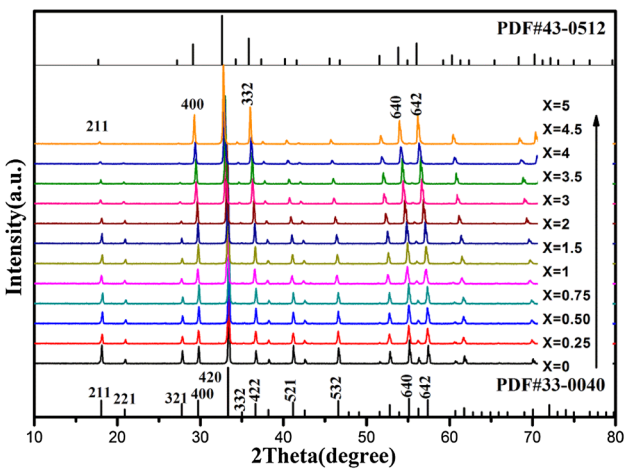

Fig. 1 XRD patterns of the $Y_{2.94}Al_{5-x}Ga_xO_{12}:Ce^{3+}_{0.06}$ (x = 0, 0.25, 0.5, 0.75, 1, 1.5, 2, 3, 3.5, 4, 4.5, 5) phosphors

Figure 2 displays the SEM images of the $Y_{2.94}Al_{5-x}Ga_xO_{12}:Ce^{3+}_{0.06}$ (x = x = 0, 0.75, 2, 3, 4, 5) phosphors. From the images, we can find that the particles of the sample replaced with a small number of the Ga^{3+} ions performs irregular shape, which consist of several small particles as shown in Fig. 2a–c. With the improvement of Ga^{3+} content, the size of individual particles increased gradually and the dispersion of the particles is getting better as shown in Fig. 2d–f. The doping of Ga^{3+} ions can help reduce the sintering temperature of YAG. Thus, the samples which content more Ga^{3+} ions are beneficial to the development of lattice.

Figure 3 shows emission spectra and excitation spectra of the $Y_{2.94}Al_{5-x}Ga_xO_{12}:Ce^{3+}_{0.06}$ (x = 0, 0.25, 0.5, 0.75, 1, 1.5, 2, 3, 3.5, 4, 4.5, 5) phosphors. The emission spectra exhibit an emission band ranging from 480 to 650 nm under the 460 nm excitation, which corresponds to the 5d → 4f transition of the Ce^{3+} ions. The results indicate that with the increasing of Ga^{3+} ions concentration, the positions of the emission peak of Ce^{3+} ions show a greatly blue-shift. Meanwhile, the luminous intensity increased gradually first and then decreased and the luminous intensity becomes the strongest when x = 0.75. When Al^{3+} ions were completely replaced by Ga^{3+} ions, the sample shows no luminescence.

To explain the phenomenon, we draw the configuration coordinate diagram of YAG:Ce^{3+}, YAGG:Ce^{3+}, and YGG:Ce^{3+}, which is showed in Fig. 4. From Fig. 4, we can find that the 5d energy level curve of Ce^{3+} will shift to the right with the increasing of Ga^{3+} ions concentration. Thus, the energy level difference between 5d and 4f in the garnet structure is YGG > YAGG > YAG. Then the luminous intensity of the samples increased with the increase of Ga^{3+} ions concentration. According to the equation of $\Delta E = h/\lambda$ (where h is Planck constant and λ is the wavelength), the λ will decrease when ΔE increased [11, 12]. But when the dopant volume of Ga^{3+} is too large, the 5D levels of Ce^{3+} are buried inside the conductance band that results in absence of Ce^{3+} luminescence in $Y_3Ga_5O_{12}:Ce^{3+}$ at room temperature [13].

As we all know, the optimal concentration of Ce^{3+} in YAGG:Ce^{3+} phosphors is affected with the ratio of Ga^{3+} to Al^{3+} [10, 12]. Figure 5 shows the emission spectra (a) and excitation spectra (b) of the $Y_{3-y}Al_{4.25}Ga_{0.75}O_{12}:Ce^{3+}_y$ (y = 0.02, 0.04, 0.06, 0.08, 0.10, 0.12, 0.14, 0.16) phosphors. The inset shows the trend of wavelength and luminous intensity with Ce^{3+} concentration. The inset indicates that with the increasing of Ce^{3+} ions concentration, the positions of the emission peak of Ce^{3+} ions show a red-shift, while the intensity increased first

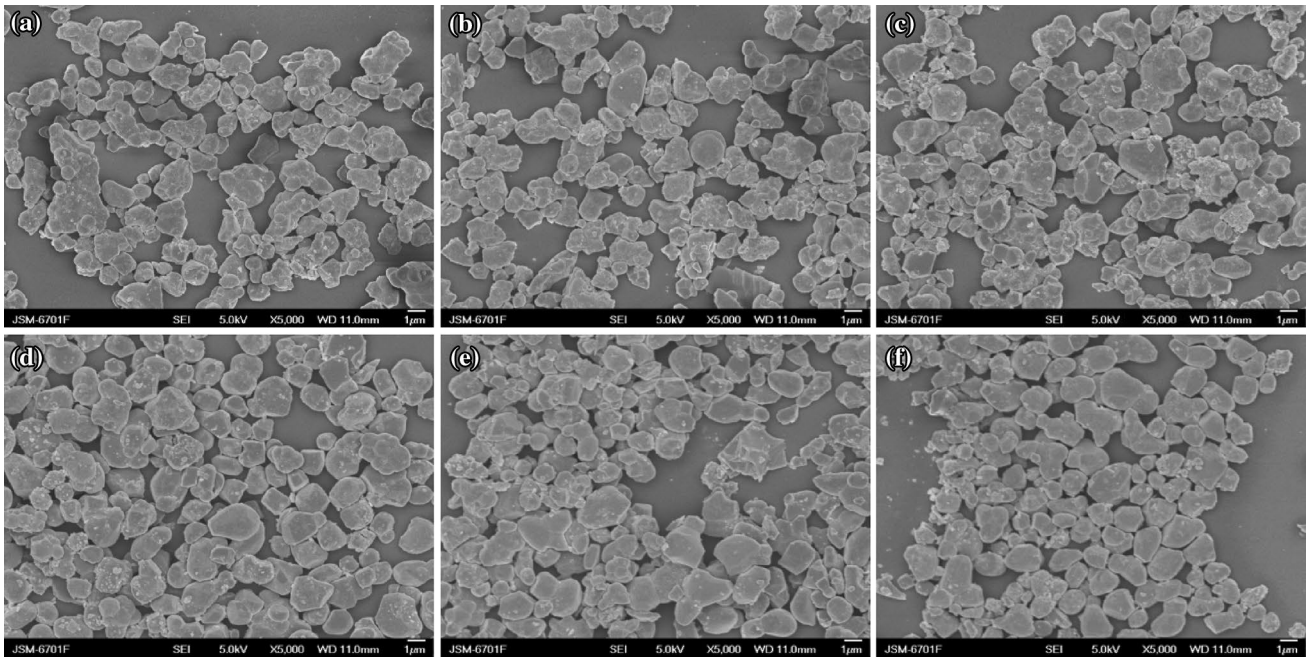

Fig. 2 SEM images of the of the $Y_{2.94}Al_{5-x}Ga_xO_{12}:Ce^{3+}{}_{0.06}$ (x = 0, 0.75, 2, 3, 4, 5) phosphors. (**a**) x = 0.0, (**b**) x = 0.75, (**c**) x = 2, (**d**) x = 3, (**e**) x = 4, (**f**) x = 5

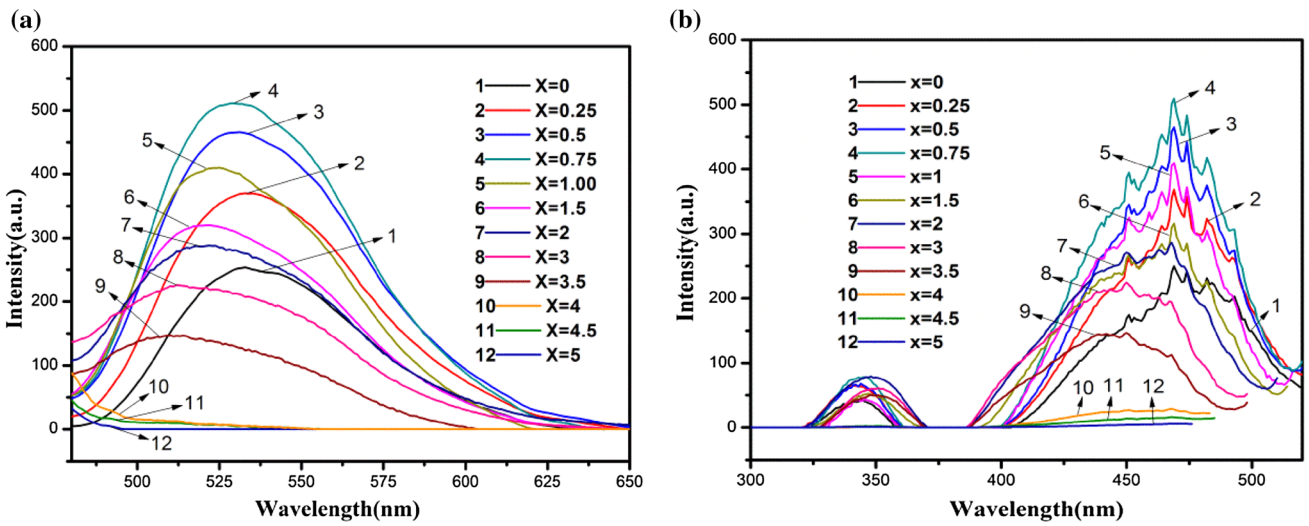

Fig. 3 Emission spectra (**a**) and excitation spectra (**b**) of the $Y_{2.94}Al_{5-x}Ga_xO_{12}:Ce^{3+}{}_{0.06}$ (x = 0, 0.25, 0.5, 0.75, 1, 1.5, 2, 3, 3.5, 4, 4.5, 5) phosphors

and then decreased, and the optimal concentration of Ce^{3+} in $Y_{3-y}Al_{4.25}Ga_{0.75}O_{12}:Ce^{3+}{}_y$ phosphors is y = 0.1.

According to the crystal field theory, the red-shift of the emission spectra of Ce^{3+} mainly depends on the splitting of the 5d levels. The crystal field splitting (Dq) can be expressed as below:

$$D_q = \frac{1}{6} Ze^2 \frac{r^4}{R^5} \quad (1)$$

where Dq represents the extent of energy level separation, Z is the charge of anion, e is the electron charge, r is the radius of the d wavefunction, and R is the bond distance between the Ce^{3+} and O^{2-}. Ga^{3+} ions with the bigger ion radius and stronger electronegativity comparing with Al^{3+} have shorter bond and the stronger interactions with the coordinate O^{2-}, which will induce the ligands of Al^{3+} sites shrinking [14–16]. So, the Dq decreases, and the emission spectra shift to longer wavelength (red-shift).

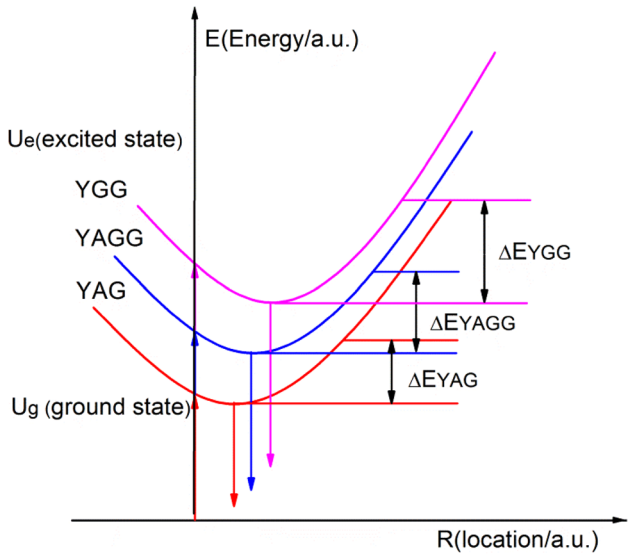

Fig. 4 Configuration coordinate diagram of YAG:Ce^{3+}, YAGG:Ce^{3+}, and YGG:Ce^{3+}

YAGG:Ce^{3+} phosphors are not only can be excited by blue light but also can be excited by cathode ray. Figure 6 shows the emission spectra of the $Y_{2.94}Al_{5-x}Ga_xO_{12}:Ce^{3+}{}_{0.06}$ (x = 0, 0.5, 0.75, 1, 1.5, 2, 3, 4, 5) and $Y_{3-y}Al_{3.5}Ga_{1.5}O_{12}:Ce^{3+}{}_y$ (y = 0.004, 0.006, 0.008, 0.01, 0.02, 0.04, 0.06, 0.08, 0.10, 0.12, 0.14) phosphors excited by cathode ray (6 kV). The results shows that the location of the emission peak is similar to the PL spectra, but the optimum concentration of the samples is x = 1.5 and y = 0.04 when they were excited by cathode ray. What's more, the cathodoluminescence intensity is much higher than that of the PL. It might be because of the energy of cathode ray is higher than blue light. All these results indicate that the YAGG:Ce^{3+} phosphors are excellent in cathodoluminescence.

Furthermore, we measured fluorescence lifetimes of Ce^{3+} in $Y_{2.94}Al_{5-x}Ga_xO_{12}:Ce^{3+}{}_{0.06}$ (x = 0, 0.75, 2, 3, 4, 5) phosphors (with emission at 535 nm upon excitation at 330 nm). As displayed in Fig. 7, it is observed that all the decay curves can be well fitted with a single-exponential equation. The lifetime increased first and then decreased with the increasing of the incorporation content of Ga^{3+} ion, which is accord with the trend of the emission intensity discussed above.

As is known, the thermal quenching is one of the important parameters for phosphors. Figure 8 displays the temperature-dependent luminescence intensity of $Y_{2.94}Al_{5-x}GaO_{12}:Ce^{3+}{}_{0.06}$ (x = 0, 0.75, 2, 3, 5) excited by 460 nm, Fig. 8f shows the trend of the normalized emission intensity. The results indicate that all intensities drop gradually with temperature increase and the decline is getting worse with the increase of the concentration of Ga^{3+}. The thermal quenching may be resulted from the two main reasons: (1) The garnet structure of $Y_{2.94}Al_{5-x}GaO_{12}:Ce^{3+}{}_{0.06}$ phosphors become more and more relaxed and rigidity gradually decreases with Ga^{3+} increasing; (2) The thermal ionization is more likely to arise as the Ga^{3+} concentration increases [17–19].

4 Conclusions

A series of $Y_{3-y}Al_{5-x}Ga_xO_{12}:Ce^{3+}{}_y$ phosphors were successfully synthesized by high temperature solid state reaction method. The diffraction angle decreased gradually with the increase of Ga^{3+} ions content because of the he lattice expansion. In PL, the critical

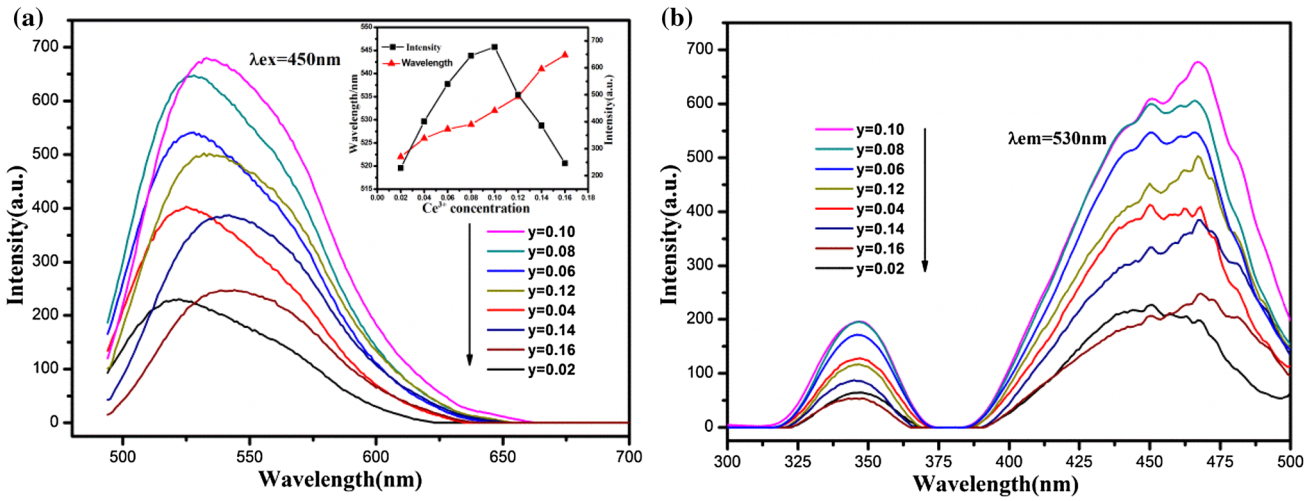

Fig. 5 Emission spectra (**a**) and excitation spectra (**b**) of the $Y_{3-y}Al_{4.25}Ga_{0.75}O_{12}:Ce^{3+}{}_y$ (y = 0.02, 0.04, 0.06, 0.08, 0.10, 0.12, 0.14, 0.16) phosphors. The inset shows the trend of wavelength and luminous intensity with Ce^{3+} concentration

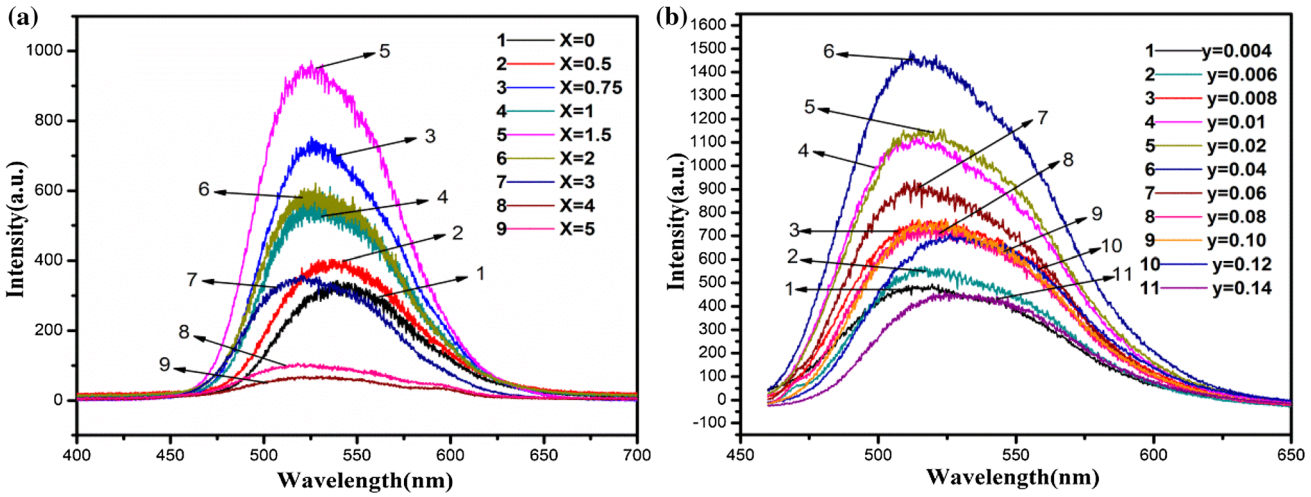

Fig. 6 Emission spectra of the $Y_{2.94}Al_{5-x}Ga_xO_{12}:Ce^{3+}_{0.06}$ (x = 0, 0.5, 0.75, 1, 1.5, 2, 3, 4, 5) (**a**) and $Y_{3-y}Al_{3.5}Ga_{1.5}O_{12}:Ce^{3+}_{y}$ (y = 0.004, 0.006, 0.008, 0.01, 0.02, 0.04, 0.06, 0.08, 0.10, 0.12, 0.14) (**b**) phosphors excited by cathode ray

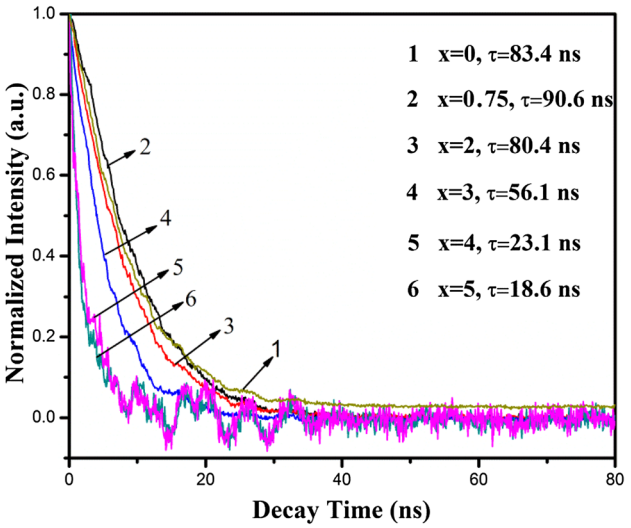

Fig. 7 Decay curves and fluorescence lifetimes of $Y_{2.94}Al_{5-x}GaO_{12}:Ce^{3+}_{0.06}$ (x = 0, 0.75, 2, 3, 4, 5) samples

concentration of Ga^{3+} ions in $Y_{2.94}Al_{5-x}Ga_xO_{12}:Ce^{3+}_{0.06}$ is x = 0.75 and the optimal concentration of Ce^{3+} in $Y_{3-y}Al_{4.25}Ga_{0.75}O_{12}:Ce^{3+}_{y}$ is y = 0.1. The fluorescence lifetimes of the $Y_{2.94}Al_{5-x}Ga_xO_{12}:Ce^{3+}_{0.06}$ phosphors showed a similar trend to the emission intensity. The temperature-dependent luminescence intensity drop gradually with temperature increase and the decline is getting worse with the increase of the concentration of Ga^{3+}. In cathodoluminescence, the optimum concentration of the samples is x = 1.5 and y = 0.04. With the improvement of Ga^{3+} content, the particle size increased gradually and the dispersion of the particles is getting better.

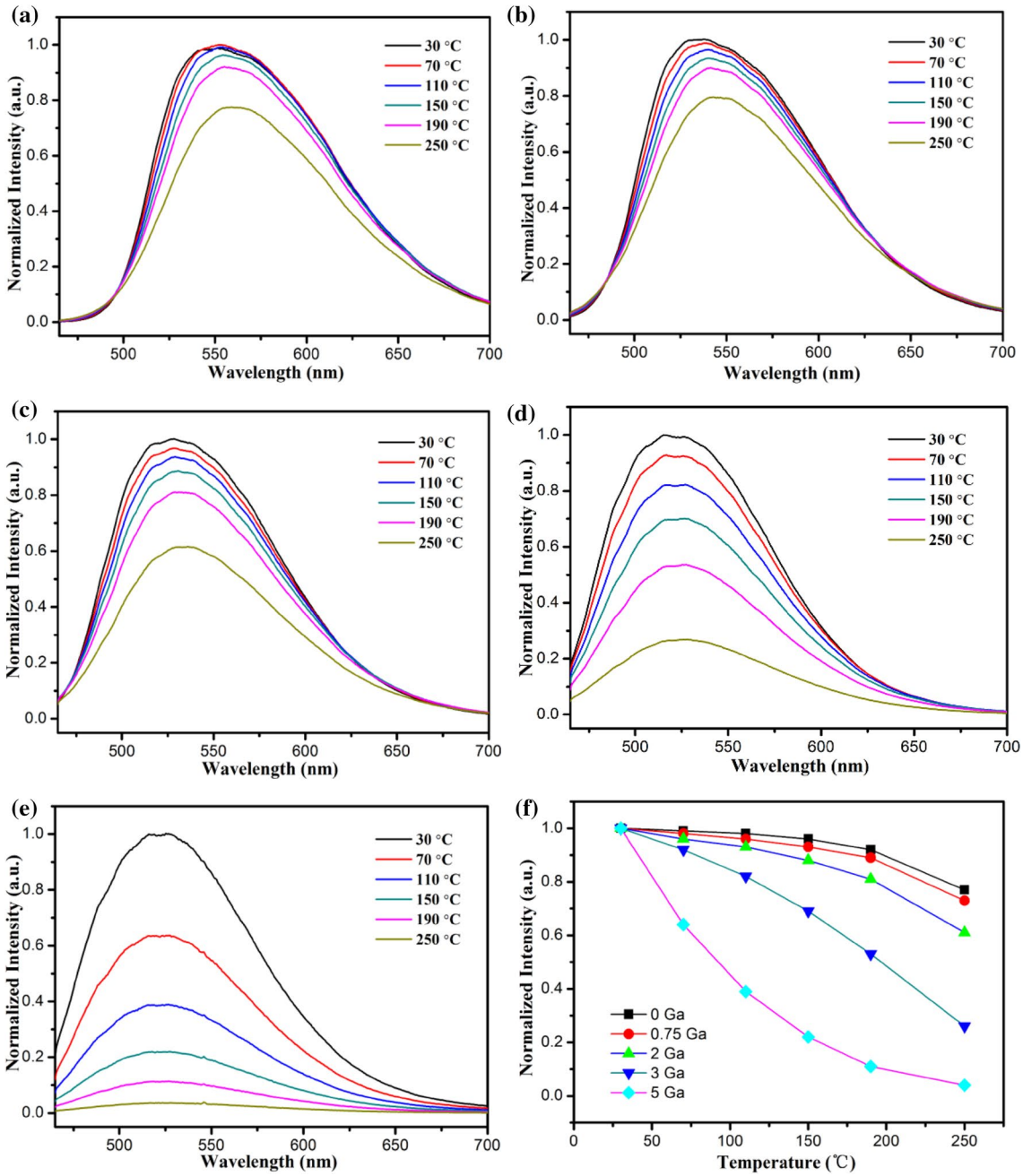

Fig. 8 Temperature-dependent luminescence intensity of $Y_{2.94}Al_{5-x}GaO_{12}:Ce^{3+}_{0.06}$. (**a**) x = 0.0, (**b**) x = 0.75, (**c**) x = 2, (**d**) x = 3, (**e**) x = 5, (**f**) shows the trend of normalized intensity

Acknowledgements This project is financially supported by the National Natural Science Foundation of China (Grant Nos. 51602027, 61307118, and 21501167), the education project of Jilin Provincial Department, China (JJKH20170607KJ). This work was supported by the "111" project of China (D17017).

References

1. J.Y. Choe, D. Ravichandran, S.M. Blomquist et al., Cathodoluminescence study of novel sol–gel derived $Y_{3-x}Al_5O_{12}:Tb_x$ phosphors. J. Lumin. **93**, 119–128 (2001)
2. V. Tucureanu, A. Matei, A.M. Avram, Synthesis and characterization of YAG:Ce phosphors for white LEDs. Opto-Electron. Rev. **23**, 239–251 (2015)

3. N. Wei, T.C. Lu, F. Li et al., Transparent Ce:YAG ceramic phosphors for white light-emitting diodes. Appl. Phys. Lett. **101**, 216–225 (2014)
4. H.L. Shi, C. Zhu, J.Q. Huang et al., Luminescence properties of YAG:Ce, Gd phosphors synthesized under vacuum condition and their white LED performances. Opt. Mater. Express **4**, 649–655 (2014)
5. M. Rejman, V. Babin, R. Kucerková et al., Temperature dependence of CIE-x,y color coordinates in YAG:Ce single crystal phosphor. J. Lumin. **187**, 20–25 (2017)
6. G. Feng, W.H. Jiang, Y.B. Chen et al., A novel red phosphor $NaLa_4(SiO_4)_3F:Eu^{3+}$. Mater. Lett. **65**, 110–112 (2011)
7. W.J. Ding, J. Wang, M. Zhang et al., A novel orange phosphor of Eu^{2+}-activated calcium chlorosilicate for white light-emitting diodes. J. Solid State Chem. **179**, 3582–3585 (2006)
8. K. Ohno, T. Abe, Effect of BaF_2 on the synthesis of the single-phase cubic $Y_3Al_5O_{12}$:Tb. J. Electrochem. Soc. **133**, 638–643 (1986)
9. M. Mori, J. Xu, G. Okada et al., Scintillation and optical properties of Ce-doped YAGG transparent ceramics. J. Rare Earth **34**, 763–768 (2016)
10. S. Fu, J. Tan, X. Bai et al., Effect of Al/Ga substitution on the structural and luminescence properties of $Y_3(Al_{1-x}Ga_x)_5O_{12}:Ce^{3+}$ phosphors. Opt. Mater. **75**, 619–625 (2018)
11. C.C. Chiang, M.S. Tsai, M.H. Hon, Luminescent properties of cerium-activated garnet series phosphor: structure and temperature effects. J. Electrochem. Soc. **155**, 2074–2078 (2008)
12. J. Ueda, S. Tanabe, T. Nakanishi, Analysis of Ce^{3+} luminescence quenching in solid solutions between $Y_3Al_5O_{12}$ and $Y_3Ga_5O_{12}$ by temperature dependence of photoconductivity measurement. J. Appl. Phys. **110**, 2–6 (2011)
13. O. Sidletskiy, V. Kononets, K. Lebbou et al., Structure and scintillation yield of Ce-doped Al-Ga substituted yttrium garnet. Mater. Res. Bull. **47**, 3249–3252 (2012)
14. M.M. Shang, J. Fan, H.Z. Lian et al., A double substitution of Mg^{2+}-Si^{4+}/Ge^{4+} for $Al_{(1)}^{3+}$-$Al_{(2)}^{3+}$ in Ce^{3+}-doped garnet phosphor for white LEDs. Inorg. Chem. **53**, 7748–7755 (2014)
15. P. Dorenbos, Crystal field splitting of lanthanide 4f 5d-levels in inorganic compounds. J. Lumin. **99**, 283 (2002)
16. J.M. Ogicglo, A. Katelnikovas, A. Zych et al., Luminescence and luminescence quenching in $Gd_3(Ga,Al)_5O_{12}$ scintillators doped Ce^{3+}. J. Phys. Chem. A **117**, 2479–2484 (2013)
17. Y.C. Qiang, Y.X. Yu, G.L. Chen et al., Synthesis and luminescence properties of $Y_{2.94}Al_{5-m}Ga_mO_{12}:0.06Ce^{3+}$ green phosphors for white LEDs. Ceram. Int. **42**, 767–773 (2016)
18. W.M. Yen, M. Raukas, S.A. Basun et al., Optical and photoconductive properties of cerium-doped crystalline solids. J. Lumin. **69**, 287–294 (1996)
19. B.B. Yang, J. Zou, F.C. Wang et al., Optical and reliability properties studies of green YAG phosphors by Ga substitution. J. Mater. Sci.: Mater. Electron. **27**, 3376–3383 (2016)